RESEARCH ARTICLE | JULY 15 2025

Toward stable multi-jet formation in ionic liquids for annular slit-type electrospray thrusters *⊙*

Chanearl Kwon (권찬얼) ⑩ ; Sunho Choe (최선호) ⑩ ; Jack J. Yoh (여재익) ☎ ⑩



Physics of Fluids 37, 072114 (2025) https://doi.org/10.1063/5.0269240





Articles You May Be Interested In

Two-scale structure of the current layer controlled by meandering motion during steady-state collisionless driven reconnection

Phys. Plasmas (July 2004)





Toward stable multi-jet formation in ionic liquids for annular slit-type electrospray thrusters

Cite as: Phys. Fluids **37**, 072114 (2025); doi: 10.1063/5.0269240 Submitted: 5 March 2025 · Accepted: 20 April 2025 ·

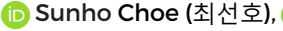
Published Online: 15 July 2025







Chanearl Kwon (권찬얼), 🕞 Sunho Choe (최선호), 🕞 and Jack J. Yoh (여재익) 🗈 🙃



AFFILIATIONS

Department of Aerospace Engineering, Seoul National University, Seoul, South Korea

^{a)}Author to whom correspondence should be addressed: jjyoh@snu.ac.kr

ABSTRACT

This study achieves stable multi-jet formation in annular slit-type electrospray emitters, focusing on the effects of viscosity and electric potential. Using water-glycerin mixtures, the transition from Taylor cone formation to multi-jet generation is analyzed. Higher viscosity is found to enhance the jet stability, enabling up to a maximum of seven stable jets at optimal conditions. Key parameters are identified as the capillary number (Ca) and Reynolds number (Re), and insights into the interplay between surface tension and viscosity are reported. The annular slit design demonstrates superior scalability and efficiency compared to the capillary emitter. Higher flow rates allow stable multi-jet formation at lower voltages, while voltages above 18.5 kV trigger instability. The reported findings provide design guidelines for optimizing electrospray systems by balancing jet stability and pulsation frequency. Sustained multi-jet formation at lower voltages improves efficiency by reducing power consumption, a critical factor for nanosatellite propulsion. High pulsation frequencies enhance thrust stability, making annular slittype emitters viable for low Earth orbit operations in microgravity environments.

Published under an exclusive license by AIP Publishing. https://doi.org/10.1063/5.0269240

NOMENCLATURE

- Capillary number Ca
- Characteristic length (m)
- Circumference of inner diameter or slit (m)
- Rayleigh charge (C) q_R
- Vonnegut charge (C)
- Reynolds number
- Cross-sectional area of the emitters' outlet (m²)
- Flow velocity (m/s)
- Δp Pressure gradient between the conductive liquid and the air
- Dielectric constant 3
- Vacuum permittivity
- Viscosity (mPa s) η
- Droplet volume (m³)
- Density (kg/m³) ρ
- Surface tension (N/m)
- Diameter of spherical drop (m)
- Electric potential (V)

I. INTRODUCTION

Electrospray technology has emerged as a critical tool in various scientific and industrial applications, ranging from satellite propulsion¹⁻¹³ to microfabrication^{14,15} and biomedical systems. 16,17

method involves the use of electric fields to ionize or disperse liquids into fine sprays of molecular ions or charged droplets, enabling precise control over thrust and mass flow. 18 In the domain of spacecraft propulsion, electrospray thrusters are particularly attractive for their ability to deliver high efficiency and precision, essential for micro- and nanosatellite operations.¹⁹ However, the advancement of this technology hinges on the development of innovative emitter designs that balance structural simplicity, operational stability, and scalability.

Among conventional emitter designs, capillary-type configurations have been widely utilized due to their simplicity and effectiveness in producing single jets. Despite their reliability, capillary emitters are limited in scalability and thrust density, as they rely on single-point emission. To overcome these limitations, a crown-type emitter configuration was introduced, leveraging multiple discrete emitters arranged radially to achieve multi-jet formation.²⁰ While this configuration increases thrust capabilities, it introduces new challenges such as fabrication complexity, high production costs, and difficulties in maintaining uniform jet stability across all emitters.

Electrostatic propulsion systems can also be classified based on propellant type and emission mechanism. Field emission electric propulsion (FEEP) thrusters, for example, use low-vapor-pressure liquid metals such as indium, gallium, or cesium, and emit ions directly from sharp emitter tips through field emission under high voltages.³ These systems typically produce sub-millinewton levels of thrust and achieve

specific impulses in the range of 4000–6000 s, making them well suited for fine attitude and orbit control applications. ^{21,22} FEEP emitters are typically categorized into needle-type, capillary-type, and slit-type. ²³ Multi-emitter configurations—like crown-type arrays or slit-based geometries—have been developed to achieve higher thrust densities by enabling multiple simultaneous emission sites. Commercial devices such as Enpulsion's IFM-Nano series employ crown-type emitters, ^{22,24} though they require intricate fabrication techniques including photolithography and electrochemical etching. ²⁵

Slit-type emitters, in contrast, offer an efficient path to dense jet generation along a continuous edge and high thrust-to-power ratios. However, their use has been limited by challenges such as beam divergence and thermal instability—particularly when using metal propellants, which may vaporize under excessive slit heating. One promising strategy is to reconfigure the emitter geometry into an annular slit. This circular design increases the effective perimeter within a compact area, enabling more uniform jet formation and potentially mitigating end-effect divergence. Although such annular slit configurations were conceptually proposed decades ago, they have not been systematically investigated or validated through experiments.

To address this gap, our prior work introduced a novel annular slit-type emitter, aiming to integrate the benefits of multi-jet capability with a simplified structure. Unlike crown-type emitters, which require multiple discrete capillary emitters, the annular slit design enables continuous jet formation along the periphery of the slit. Recent experimental results demonstrated that this design could produce up to seven stable jets using water and glycerin as working fluids under the atmospheric condition. These results revealed key challenges, including jet instability at higher voltages and sensitivity to operational parameters such as fluid viscosity and flow rate, highlighting the need for thorough and comprehensive parametric studies that lead to the practical operation of an electrospray thruster. Then, the findings highlighted the need for further optimization and a deeper understanding of the underlying mechanisms governing multi-jet formation and stability.

The present study advances the investigation of annular slit-type emitters by addressing critical challenges. Specifically, this research focuses on exploring the effects of water-glycerin mixtures with varying viscosities and electrical properties to better understand the factors influencing jet stability and efficiency. The study introduces a new experimental setup that allows for precise control and monitoring of electrospray phenomena under a broader range of operating conditions, including higher voltages and flow rates. High-speed imaging and advanced analysis techniques are utilized to capture the dynamics of jet formation, shedding light on the transitions between different electrospray modes. To establish a framework for optimizing the annular slit-type emitter's performance, the relationship between operational parameters and the spatial distribution of jets is analyzed by identifying conditions that minimize interference and maximize uniformity. Unlike the prior studies that primarily focused on demonstrating the feasibility of the annular slit design, 12 this work delves into the mechanism of multi-jet interactions, investigating how electric field distributions and fluid properties contribute to stability and performance. Additionally, this study aims to quantify the tradeoffs between thrust efficiency and system complexity. The annular slit-type emitter offers potential advantages in terms of manufacturing and operational simplicity compared to crown-type emitters, which require intricate

assembly processes. The investigation also incorporates a comparative analysis of capillary and annular slit-type emitters, emphasizing their respective strengths and limitations. This comparison is critical for identifying the contexts in which annular slit-type emitters provide clear advantages, such as applications requiring higher thrust densities or improved scalability.

The relevance of this study to nanosatellite propulsion is particularly significant. The ability of annular slit-type emitters to generate multiple stable jets at lower voltages directly contributes to electrospray thruster efficiency by reducing power consumption—a critical factor in nanosatellite systems with limited power budgets. Additionally, the high-frequency pulsating jet behavior observed in certain regimes enhances thrust stability, enabling precise attitude control and maneuverability in space. In the multi-jet regime, however, the jets exhibited highly stable and steady emission with no measurable pulsation frequency. While this prevented direct frequency analysis, the absence of pulsation suggests excellent temporal thrust uniformity, which is favorable for precise spacecraft control. This stability may also help avoid interference with control bandwidths, supporting fine maneuvering capabilities. This multi-jet capability also opens new avenues for applications such as precision manufacturing, inkjet printing, and precise drug delivery systems.

II. THEORY ON THE TAYLOR CONE FORMATION AND MULTI-JET FORMATION

The formation of Taylor cones and subsequent multi-jet emission in electrospray systems is driven by the interaction of electrostatic forces, surface tension, and viscosity. These parameters collectively influence the stability and dynamics of cone–jet transitions, which are essential for multi-jet formation.

A. Taylor cone formation

A Taylor cone forms when the electric stress at the liquid–air interface surpasses the restoring forces of surface tension. This balance is described by

$$\gamma \nabla \cdot n - \frac{1}{2} \varepsilon (\nabla \phi)^2 = \Delta p, \tag{1}$$

where n is the surface in the direction of the air, $\nabla \cdot n$ is the curvature, ϕ is the electric potential which is the emitter voltage, and Δp is the pressure gradient between the conductive liquid and the air. The critical charge required for instability leading to cone formation is given by the Rayleigh and Vonnegut charge equations,

$$q_R = \pi \left(2\varepsilon \sigma \emptyset_D^3 \right)^{\frac{1}{2}},\tag{2}$$

$$\frac{q_V}{V} = 6\left(2\varepsilon\sigma\emptyset_D^{-3}\right)^{\frac{1}{2}}.\tag{3}$$

Here, q_R is the Rayleigh charge, q_V/ν is the Vonnegut charge divided by droplet volume, ε is the dielectric constant, σ is the surface tension of the liquid, and \emptyset_D is the diameter of the spherical drop.³⁰ These charges mark the threshold at which the liquid interface destabilizes to form jets.

B. Influences of surface tension and viscosity

The interplay between surface tension and viscosity plays a critical role in determining jet stability and multi-jet formation.

This relationship is captured by the dimensionless numbers such as Capillary number (Ca) and Reynolds number (Re),

$$Ca = \frac{\eta u}{\sigma}, \tag{4}$$

$$Re = \frac{\rho uL}{\eta},\tag{5}$$

$$L = \frac{4 \times s}{l},\tag{6}$$

where σ is surface tension, η is viscosity, ρ is fluid density, u is flow velocity, L is a characteristic length, s is cross-sectional area of the emitters' outlet, and l is circumference of inner diameter or slit. When Ca is low, surface tension dominates, leading to fewer, more stable jets. However, when Ca is high, viscosity becomes significant, enabling higher stability in multi-jet modes, especially in high-viscosity fluids like glycerin.

In contrast, the Re represents the balance between inertial and viscous forces in the fluid. Higher Re values indicate a greater influence of inertial forces, leading to increased flow instability and jet breakup, whereas lower Re values suggest a flow dominated by viscosity, which can help stabilize the jets. In the case of annular slit-type emitters, the presence of multi-jet is influenced by both Ca and Re, where an optimal range of Re ensures stable jet formation without excessive droplet detachment or chaotic oscillations. Thus, while Ca determines the likelihood of multi-jet formation, Re dictates the stability and transition dynamics of these jets under varying operating conditions.

C. Multi-jet formation mechanism

The formation of emission sites in slit emitters follows wave-like instabilities on the liquid surface under an applied electric field. The spacing between jets (λ) is determined by the balance between surface tension (σ) and electrostatic forces caused by the electric field (E_0), given by the characteristic instability wavelength,

$$\lambda = \frac{2K\pi\sigma}{\varepsilon_0 E_0^2},\tag{7}$$

$$E_0 = (2\sigma/\varepsilon_0 r_0)^{1/2}. (8)$$

Here, K is 1 or 10, and ε_0 is the vacuum permittivity. As the voltage increases, E_0 increases, reducing λ and allowing more emission sites to form. However, beyond a certain threshold, jet merging and charge repulsion effects lead to instability, which limits the number of stable jets.

The annular slit emitter effectively acts like a closed-loop slit emitter, where jets form at periodically spaced emission sites around the slit circumference. The total number of jets N depends on the emitter perimeter L and the instability wavelength λ , 2

$$N = \frac{L}{\lambda}. (9)$$

For a given slit length, the maximum possible number of jets is determined by the minimum stable emission site spacing (λ). As the voltage increases, λ decreases, and more jets can form, but only up to a certain limit before instabilities form. Applying the derived equation to the glycerin used in this study and the cylindrical slit emitter, the calculated number of jets was 7.8 when the slit length was 12.56 mm. The experimental results showed the formation of seven jets,

demonstrating a strong agreement between the theoretical calculations and the experimental observations.

Higher viscosity fluids, such as glycerin-water mixtures, exhibit greater resistance to shear stresses caused by fluctuations in fluid flow and electric forces, stabilizing the multi-jet configuration. However, excessive emission sites lead to flow competition, which disturbs uniformity and forces weaker jets to collapse. In the current study, the combination of emitter geometry (annular slit), electrohydrodynamic jet spacing constraints, electrostatic repulsion between adjacent jets, and fluid properties (viscosity and surface tension) result in seven jets for this configuration.

D. Implications for annular slit-type emitters

The annular slit-type emitter demonstrates superior multi-jet performance compared to traditional capillary emitters due to its geometry. At an optimal potential (e.g., 18.5 kV for glycerin), up to seven stable jets are formed, distributed symmetrically around the slit. Beyond this voltage, instability due to excessive electrostatic forces reduces jet numbers. This interplay between viscosity, surface tension, and electric field strength underpins the emitter's ability to achieve high thrust efficiency with stable multi-jet configurations.

III. MATERIALS AND METHODOLOGY

A. Experimental setup

Figure 1 illustrates the experimental setup designed to investigate electrospray phenomena under atmospheric conditions using various emitter types. The configuration is modeled after the concept proposed by Kwon *et al.*, ¹² consisting of an emitter and an accelerator mounted on an acrylic holding plate. The emitter is oriented vertically upward, while the accelerator is a simple aluminum extractor plate with a circular aperture positioned horizontally. To evaluate the electrospray prototype, water–glycerin mixtures were used as working fluids in an open-air environment.

The setup includes a push-fit mechanism to facilitate easy switching between different emitter configurations. The distance between the emitter tip and the extractor hole can be adjusted by repositioning the extractor on the retaining plate using screw-and-tighten arrangements. The emitter and the extractor are connected to the high-voltage power supply, with the positive terminal linked to the emitter and the negative terminal to the extractor. The negative terminal of the extractor was maintained at ground potential during all experiments to ensure a stable electric field configuration. A steady low flow rate of the working fluid is maintained via a non-conductive conduit connecting the emitter body to the fluid input source. A syringe pump, with a capacity ranging from 1 μ m/min to 150 mm/min and an accuracy of \pm 0.5%, regulates the flow rate, ensuring smooth and pulsation-free delivery of the working fluid. The pump was calibrated for the different fluid mixtures used in this study.

Flow rates of 30 and 55 cc/h were used to ensure stable jet formation, particularly for high-viscosity mixtures like the 100% mixture (glycerin). Although these rates are higher than those typically used in ionic liquid-based electrospray thrusters (1–5 cc/h per emitter), they were chosen to enable clear observation of multi-jet dynamics and maintain operational stability under atmospheric conditions.

A high-speed camera (PHANTOM V711, featuring a 1280×800 CMOS sensor) equipped with a miniature zoom lens (focal length $105\,\text{mm})$ and illuminated by an LED light source was employed to

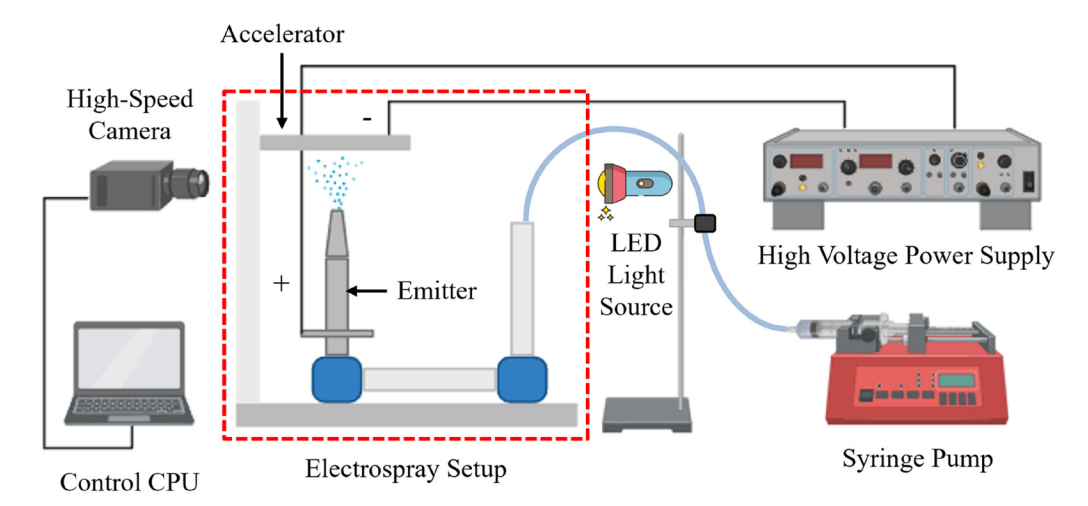


FIG. 1. Schematic of experimental setup.

capture the transition from Taylor cone formation to steady jet development. The camera recorded time-resolved shadow spraying images at a frame rate of 10 000 frames per second, with a gate time of 1.0 μ s, at intervals of 100 μ s for subsequent analysis. All experiments were conducted under controlled atmospheric conditions, with a temperature of 20 °C and a pressure of 1 atm. These conditions were selected to enable controlled evaluation of jet behavior and emitter performance, with water–glycerin mixtures serving as a surrogate for ionic liquids in early-phase testing. An in-house algorithm was used to process and analyze the captured images.

B. Emitter configuration

Figure 2 illustrates the dimensional specifications of the two emitter configurations employed in this study. The first configuration is a capillary emitter, which has a diameter of 2 mm and a length of 115 mm, representing a conventional design that has been extensively studied in prior research as shown in Fig. 2(a). To facilitate electrical connection, a disk-shaped structure with a diameter of 30 mm is integrated into the setup. The second configuration is an innovative annular slit-type emitter, explored in this study for its novel design and functionality. As depicted in Fig. 2(b), this emitter has a height of 113 mm, an inner diameter of 4 mm, and a slit thickness of 0.5 mm. Additionally, a central hole with a diameter of 3 mm is incorporated into the annular slit to enable drainage of liquids flowing toward the center. Similar to the capillary emitter, a 30-mm-diameter disk is positioned 30 mm from the bottom edge to assist in establishing an electrical connection.

C. Working fluids

In the current experiment, a variety of water-glycerin mixtures were used as working fluids for atmospheric testing. The transition from cone to jet formation, along with the subsequent flow interactions, is strongly affected by the physical properties of these liquids.

In this study, water-glycerin mixtures were selected as surrogate working fluids for electrospray thruster experiments. This selection is motivated by their tunable physical properties, particularly viscosity and surface tension, which are critical to electrospray behavior. Glycerin's high viscosity and low vapor pressure enable stable jet formation and suppress evaporation under atmospheric conditions, whereas water provides lower viscosity and higher surface tension, allowing broader exploration of electrospray regimes. Furthermore, the range of electrical conductivities and permittivities of water–glycerin mixtures qualitatively resemble those of ionic liquids used in practical electrospray propulsion systems. Therefore, they provide an effective experimental proxy for understanding cone–jet transitions, pulsation behavior, and jet stability in conditions analogous to those in space propulsion applications.

In addition to viscosity and surface tension, the electrical properties of the water–glycerin mixtures—namely, conductivity and relative permittivity—also vary with composition. As the glycerin concentration increases, both conductivity and permittivity decrease, which in turn affects charge relaxation behavior and the electric field distribution near the emitter. These changes influence the onset of jet formation and the stability of the cone–jet mode.

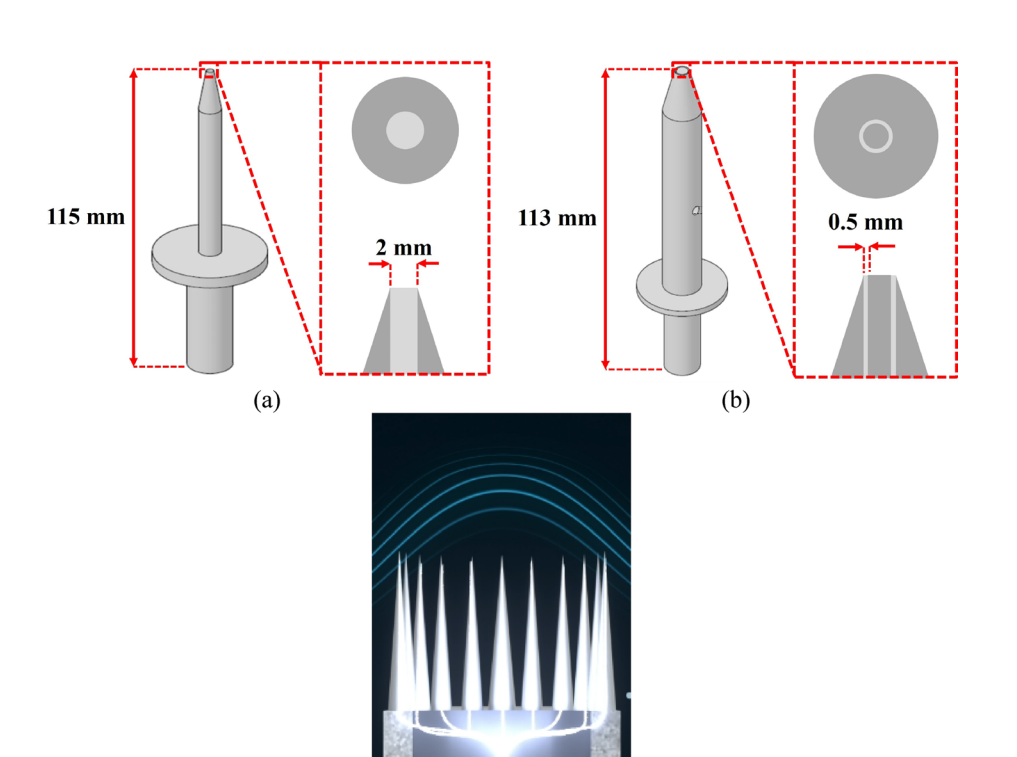
Table I presents the electrical and physical properties of the working fluids under investigation.

IV. RESULTS AND DISCUSSION

A. Capillary-type emitter

1. Hydrodynamic mode

The observed diameters of water–glycerin mixture drops generated by a capillary-type emitter at various applied voltages are presented in Fig. 3. Figure 3(a) demonstrates that drop sizes increase with applied voltage within the dripping mode. In this mode, the gravitational force is dominant over the electromagnetic force, resulting in the observed behavior. As the applied voltage increases, the stronger electric force inhibits drop detachment, leading to larger drop sizes. For instance, as shown in Fig. 3(b), the diameter of the drop from the 15% mixture is 4.0 mm at an applied voltage of 4 kV, increasing to 4.8 mm as the voltage rises to 10 kV. Additionally, at the same applied voltage, the drop sizes for the 15% and 30% mixtures are larger than those of the 0% mixture. However, when comparing the two mixtures,



(c)

FIG. 2. Schematic of different emitter configurations: (a) capillary-type, (b) annular slit-type (this work), and (c) crown needle-type.

the drop size of the 15% mixture is greater than that of the 30% mixture, as illustrated in Fig. 3(b). This indicates that as viscosity increases, drop size also increases; however, beyond a certain point, excessive viscosity results in smaller drop sizes in the dripping mode.

2. Cone-jet mode

A pulsating jet, marked by an alternating transition between cone and jet, was observed in a capillary-type emitter with 0%–60% mixtures as the electric potential increased. At higher voltages (10–11 kV), this mode shifted to a whipping emission, with jets alternately forming on either side of the emitter, as shown in Fig. 4(a). When the voltage exceeded 13 kV, the rapid alternation created the appearance of two continuous jet streams. For the 60% mixture, a thin and elongated jet formed along with the cone, and a whipping jet was observed at the end of the jet, as illustrated in Fig. 5. This whipping jet subsequently detached from the cone and transitioned into discrete droplets, highlighting the complex dynamics of jet formation and detachment at higher viscosities and electric potentials.

TABLE I. Physical properties of the water-glycerin mixtures. 33,34

3. Effect of viscosity on droplet size

Figure 6 depicts the droplet diameters resulting from jets detaching from the emitter meniscus. As the applied voltage increases, the droplet diameter decreases due to the heightened electric charge, which accelerates droplet formation near the emitter outlet during pulsating jet modes. At higher flow rates, the effects of viscosity become more pronounced. Figure 6(a) shows that at lower flow rates, the trend of droplet size variation with respect to liquid mixture ratio is less distinct. This is because at low flow rates, the effects of viscosity are less dominant, and surface tension variations among different mixtures do not significantly alter the droplet formation process. Additionally, the slower jet detachment rate reduces the influence of viscosity on droplet size differentiation.

In contrast, Fig. 6(b) demonstrates that at higher flow rates, an increase in glycerin concentration leads to a more pronounced trend of larger droplet sizes at the same voltage. This behavior arises because higher glycerin content results in greater viscosity, which correlates with increased surface tension, making droplets less susceptible to

Mixture ratio	Density (kg/m³)	Surface tension (mN/m)	Viscosity (mPa s)	Conductivity (S/m)	Relative permittivity
0% (Water)	1000	72.6	1.131	0.02-0.08	80
15%	1040	71.4	1.537	1.5-2.0	65-73
30%	1073	70.8	2.227	1.0-1.5	55-62
60%	1154	68.3	10.81	0.6-1.0	40-48
100% (Glycerin)	1261	63.4	954	1.0	17-74.32

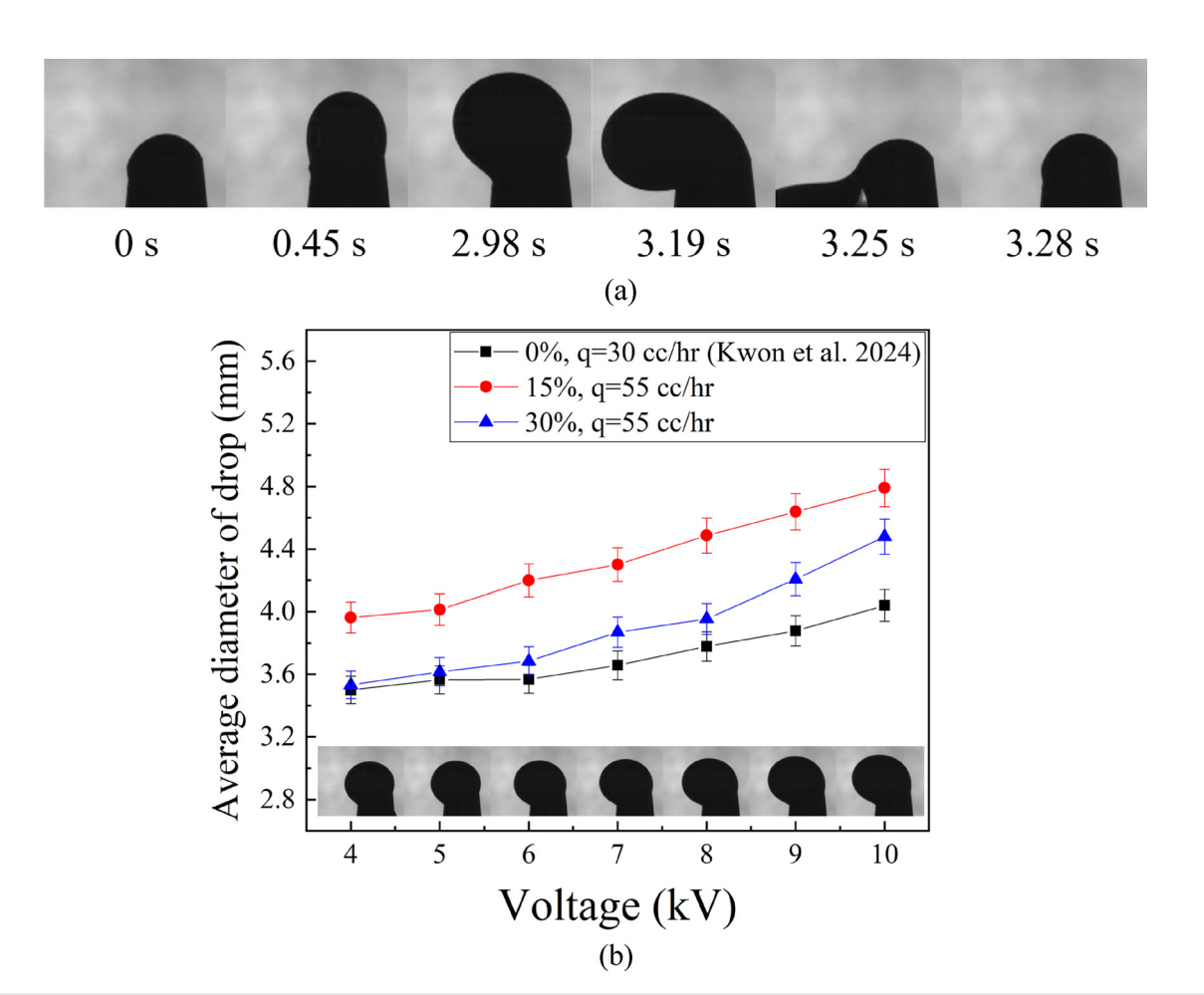


FIG. 3. (a) Time sequential images of one cycle with a capillary-type emitter illustrating the dripping mode of 15% water–glycerin mixture at 10 kV and (b) average diameter of water–glycerin mixtures' drop with voltage in a capillary-type emitter.

deformation and breakup. Consequently, at high flow rates, the impact of viscosity on droplet formation becomes more significant, leading to a clear trend where higher glycerin concentrations produce larger droplets. This interplay between voltage, flow rate, and viscosity highlights the complex dynamics of droplet formation and the significant role physical properties play in determining droplet behavior.

4. Effect of viscosity and flow rate on pulsating jet frequency

During the cone-jet mode, a jet formed by 0%-60% mixtures detaches from the emitter meniscus and transitions into micro-sized droplets. The figure demonstrates the relationship between the applied voltage and the pulsating jet frequency of the water-glycerin mixture. It is observed that the pulsating jet frequency of jet formation increases with higher applied voltage, with this effect being more pronounced at greater flow rates. However, at the same voltage, the pulsating jet frequency decreases as viscosity increases. This indicates that higher viscosity dampens the rate of jet formation, likely due to the increased resistance to flow and deformation in more viscous mixtures. This decrease in pulsating jet frequency occurs because the greater viscosity

of the mixture increases droplet size and delays its separation from the meniscus. Since pulsating jet frequency is directly related to thrust stability, the experimental results confirm that lower viscosity leads to higher frequencies, thereby enhancing thrust stability.

In addition, the comparative results for flow rates of 30 and 55 cc/h are also presented in Fig. 7. For the 0% mixture, the pulsating jet frequency is similar at both flow rates. However, for mixtures with 15%, 30%, and 60% glycerin content, the pulsating jet frequency increases with higher flow rates. This behavior can be attributed to the dynamics of droplet formation: at lower flow rates, droplets take longer to reach the critical size required for separation, resulting in a lower pulsating jet frequency. Conversely, higher flow rates accelerate droplet formation and separation, leading to an increase in pulsating jet frequency. Thus, higher flow rates provide greater thrust stability due to the higher pulsating jet frequency.

B. Annular slit-type emitter

To evaluate the geometric influence on electrospray behavior, the same experimental procedures were applied to the annular slit-type emitter. Sections IVB1 and IVB2 present the results obtained

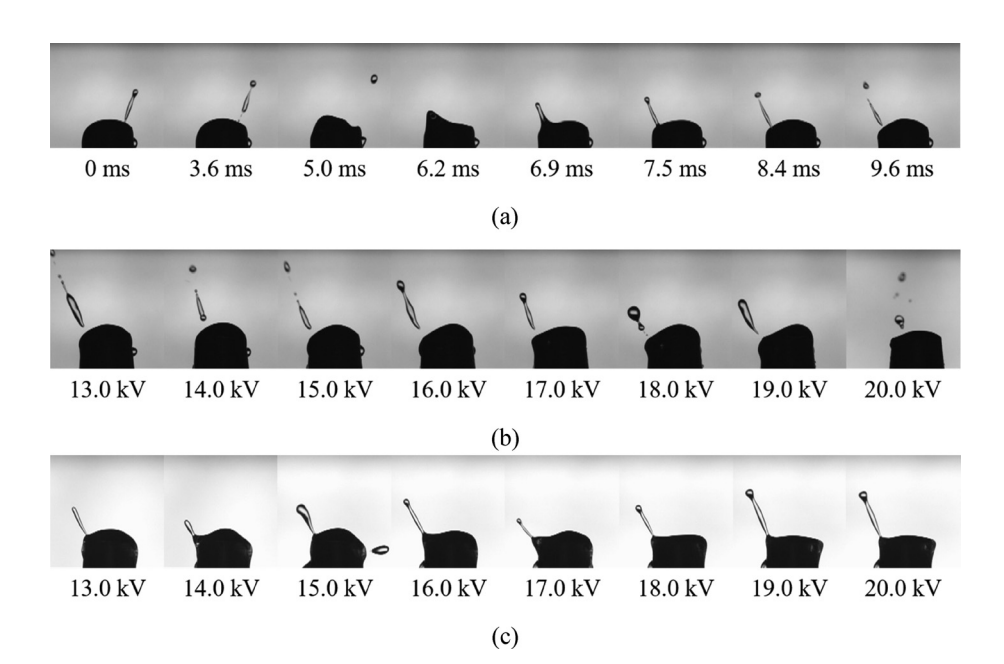


FIG. 4. (a) Time sequential images of jet formation of 15% water–glycerin mixture in capillary-type emitter at 15 kV, (b) formation of pulsating jet of 15% water–glycerin mixture with increasing voltage, and (c) formation of pulsating jet of 30% water–glycerin mixture with increasing voltage.

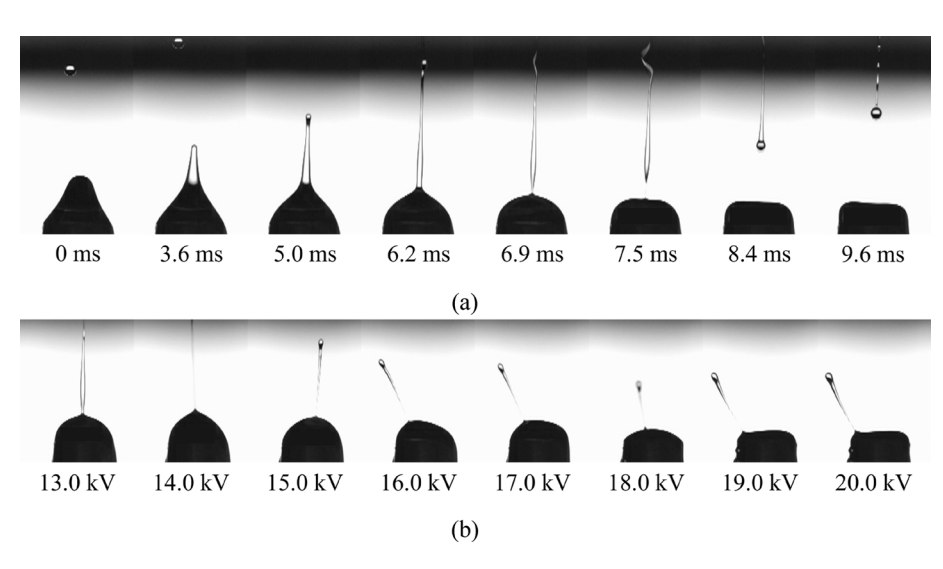


FIG. 5. (a) Time sequential images of jet formation of 60% water–glycerin mixture in capillary-type emitter at 13 kV and (b) formation of pulsating jet of 60% water–glycerin mixture with increasing voltage.

from this configuration before making comparisons with the capillary emitter.

1. Effect of viscosity on droplet size and pulsating jet frequency

Figure 8(a) presents a time-sequenced visualization of one complete pulsation cycle at 15 kV for the 15% water–glycerin mixture. The images show the evolution of the cone–jet structure from the initial cone formation to jet ejection and droplet detachment, highlighting the characteristic pulsating behavior of the annular slit emitter. In contrast, Fig. 8(b) presents snapshots of the 15% mixture at varying voltages (13–20 kV), captured at similar time frames (4.1 ms), illustrating how the cone–jet structure evolves with increasing voltage. After

achieving the necessary cone–jet length, this phenomenon occurs as the forces within the system cause the jet to split and disperse. This process resembles the behavior observed in capillary emitters, which are characterized by a repeated cycle of transitions between cone-to-jet and jet-to-droplet configurations. These transitions result in the formation of a pulsating water jet that mirrors the oscillatory patterns seen in the capillary emitter systems, as shown in Figs. 8 and 9.

For the 60% mixture, a thin and elongated jet formed along with the cone, and a whipping jet was observed at the end of the jet similar to the case of capillary-type emitter, as illustrated in Fig. 10. This whipping jet subsequently detached from the cone and transitioned into discrete droplets, highlighting the complex dynamics of jet formation and detachment at higher viscosities and electric potentials, as shown in Fig. 10(a). A slender, extended jet formed in conjunction with the

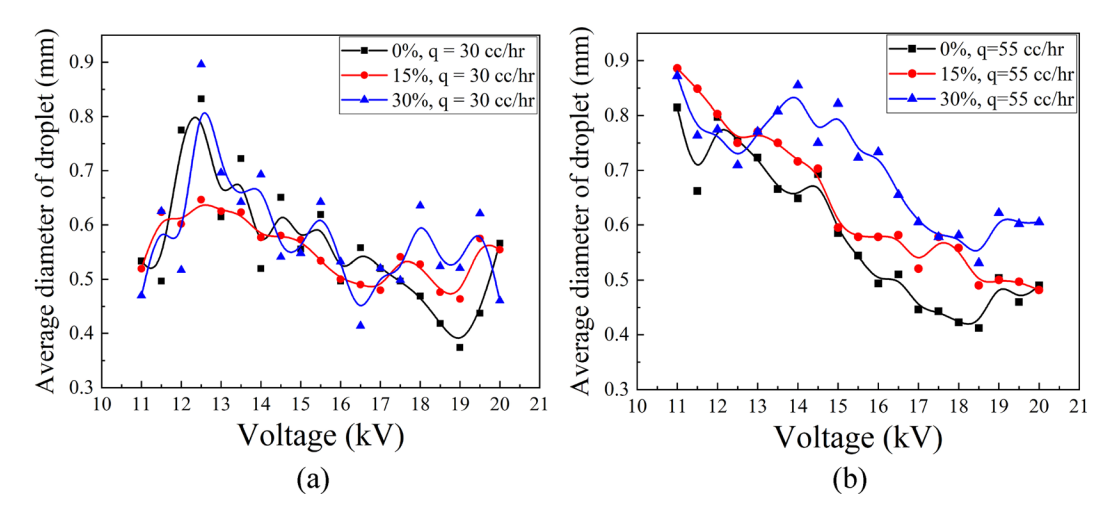


FIG. 6. Average diameter of water-glycerin mixture droplets during pulsating jet mode with voltage in a capillary-type emitter and flow rate of (a) 30 cc/h and (b) 55 cc/h.

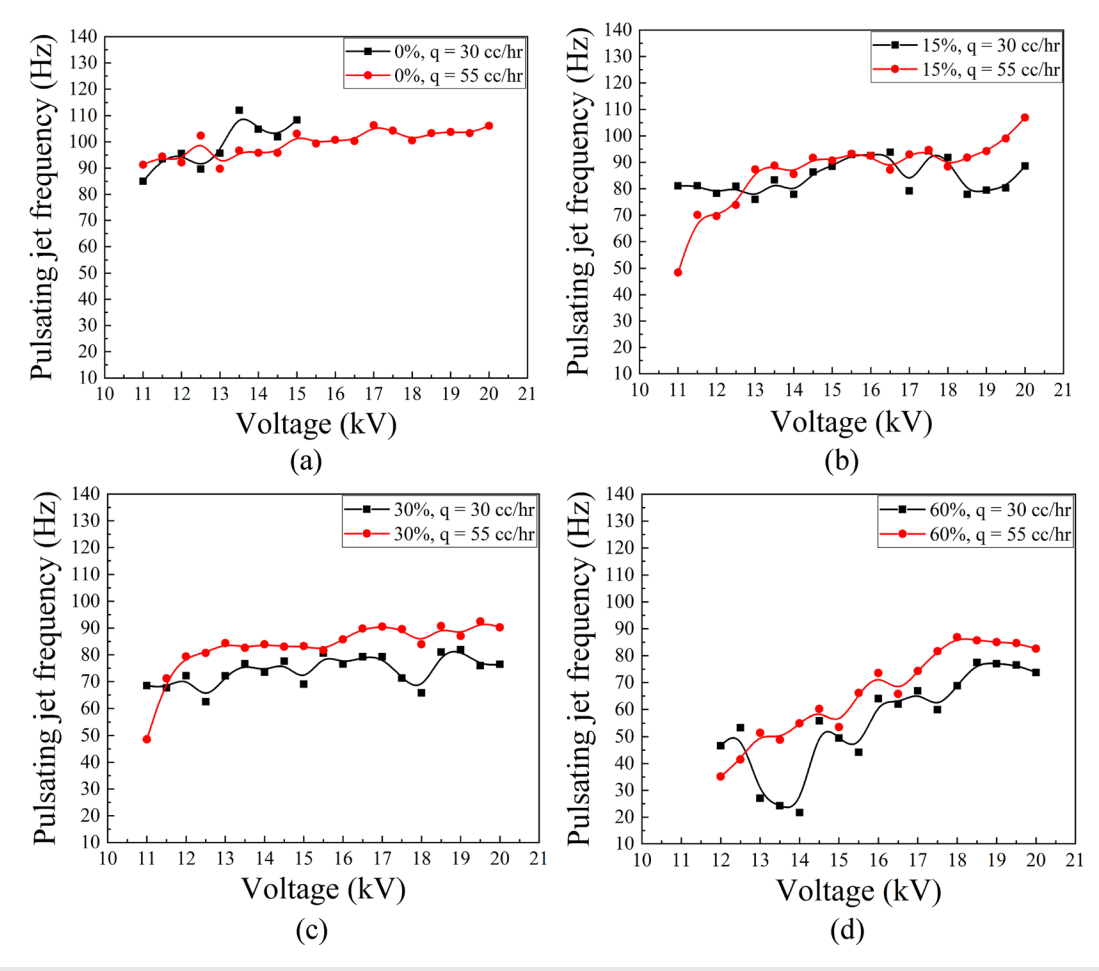


FIG. 7. Comparison of pulsating jet frequency of water–glycerin mixture droplets during pulsating jet mode with voltage in a capillary-type emitter per flow rates: (a) 0% mixture, (b) 15% mixture, (c) 30% mixture, and (d) 60% mixture.

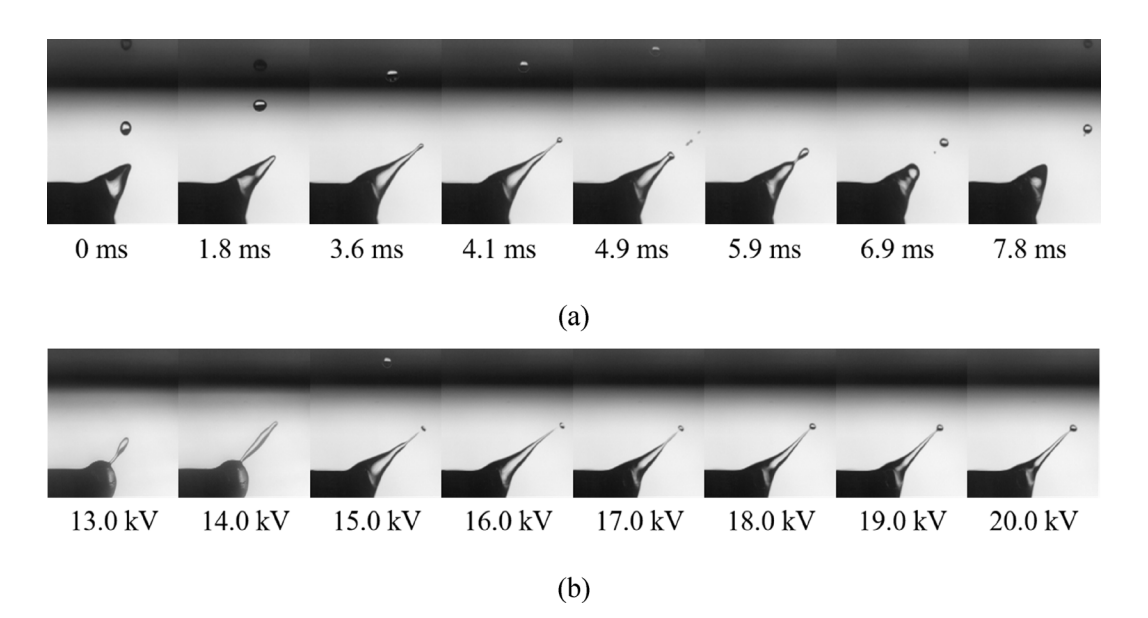


FIG. 8. (a) Time sequential images of jet formation of 15% water–glycerin mixture in annular slit-type emitter at 15 kV and (b) formation of pulsating jet of 15% water–glycerin mixture with increasing voltage.

cone for the 60% mixture. At the jet's tip, a whipping motion was observed, comparable to the behavior seen with capillary-type emitters. The complex dynamics of jet generation and detachment under higher viscosities and electric potentials were evident when this whipping jet eventually separated from the cone and transitioned into distinct droplets.

In the cone-jet mode, higher voltages accelerated droplet formation at the emitter outlet, leading to a reduction in droplet diameter, consistent with observations from capillary-type emitters. Additionally, at the same voltage, droplet size increased with viscosity, as observed with the capillary-type emitter, as shown in Fig. 11(a). However, in terms of pulsating jet frequency, the 15% and 30% mixtures exhibited lower values compared to the 0% and 60% mixtures, as shown in Fig. 11(b). The higher frequency observed in the 0% mixture (pure water) is due to its low viscosity and high surface tension, which allow the liquid to respond dynamically to the electric field, resulting in faster pulsations. For the 60% mixture, despite its high viscosity, the lower surface tension facilitates rapid droplet detachment once jets are

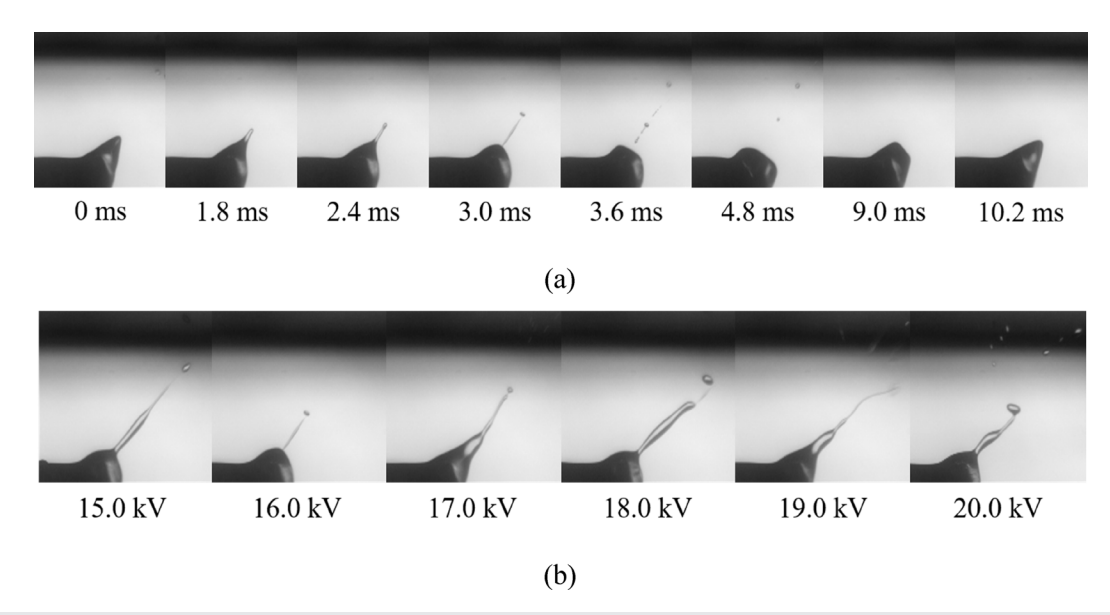


FIG. 9. (a) Time sequential images of jet formation of 30% water–glycerin mixture in annular slit-type emitter at 16 kV and (b) formation of pulsating jet of 30% water–glycerin mixture with increasing voltage.

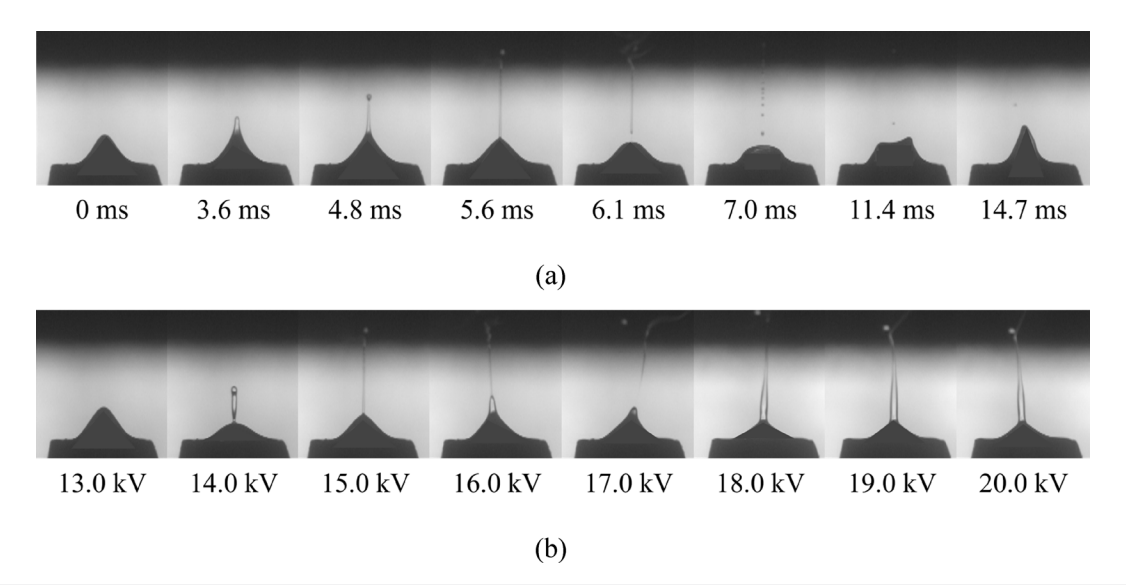


FIG. 10. (a) Time sequential images of jet formation of 60% water–glycerin mixture in annular slit-type emitter at 15 kV and (b) formation of pulsating jet of 60% water–glycerin mixture with increasing voltage.

formed, while the viscosity stabilizes the jets, supporting higher frequencies. In contrast, the 15% and 30% mixtures have intermediate viscosity and surface tension, which do not provide the optimal balance for either rapid detachment or jet stability, leading to lower pulsating jet frequencies.

The difference in pulsating jet frequency trends between capillary-type and annular slit-type emitters, as seen in Fig. 11(b), can be attributed to their geometries and how they distribute electric forces. In capillary-type emitters, the electric field is concentrated at a single point, making the system more sensitive to viscosity, which slows down droplet detachment and reduces pulsating jet frequency as glycerin content increases. Conversely, annular slit-type emitters distribute the electric field evenly along the circular slit, enabling the formation of multi-jet. This geometry reduces the dominance of viscosity

in slowing jet pulsation and stabilizes the system even at higher glycerin concentrations. Thus, in annular slit-type emitters, the distributed electric field and multi-jet formation support higher frequencies for high-viscosity mixtures, such as 60%, while intermediate mixtures (15% and 30%) do not achieve the same stability due to their suboptimal balance of viscosity and surface tension. As previously explained, higher pulsating jet frequency enhances thrust stability, indicating that the 0% and 60% mixtures provide superior thrust stability. The reduced pulsation frequency observed in the 15% and 30% mixtures may be attributed to non-ideal molecular interactions between water and glycerin, which can create local interfacial tension gradients or alter the charge relaxation dynamics. These effects could delay the charge buildup required for jet emission, resulting in longer pulsation cycles.

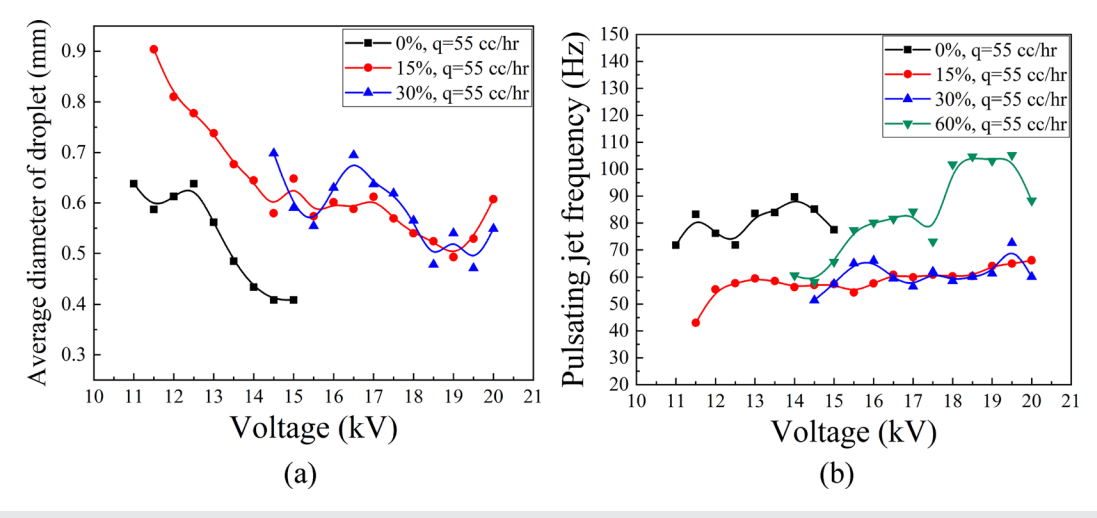


FIG. 11. (a) Average diameter and (b) pulsating jet frequency of water-glycerin mixture droplets during pulsating jet mode with voltage in an annular slit-type emitter.

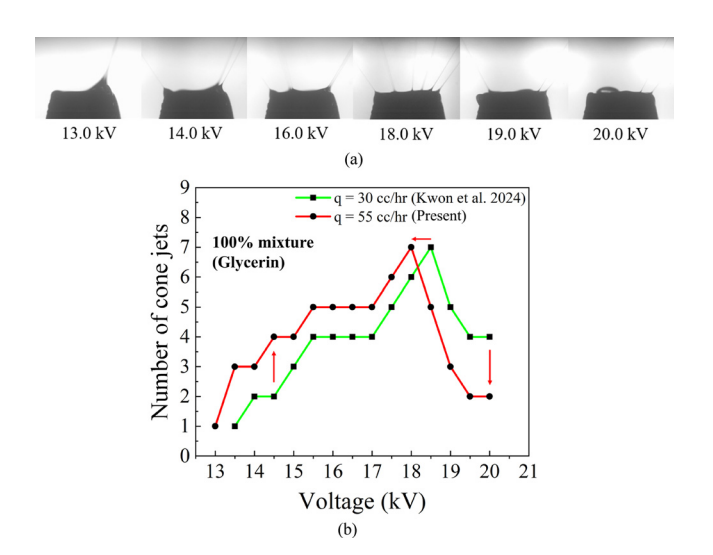


FIG. 12. (a) Formation of steady multi-jet of 100% mixture (glycerin) with voltages at 13–20 kV and flow rate of 55 cc/h and (b) variation of number of jets of 100% mixture (glycerin) with voltage and flow rate.

In the case of the 100% mixture (glycerin), pulsating behavior was not observed due to the extremely high viscosity. However, the jet remained steady and stable, suggesting that thrust stability in high-viscosity regimes can be achieved through viscous damping rather than high-frequency pulsation. This indicates the existence of two distinct mechanisms for achieving thrust stability: high pulsation frequency in low-viscosity fluids and strong viscous damping in high-viscosity fluids.

2. Effect of flow rate

For the 100% mixture (glycerin), as the applied voltage increased from 13 to 18.5 kV, the electrospray mode transitioned from a single jet to crown-like multi-jet. At 13.5 kV with a flow rate of 30 cc/h, the first jet emerged, initiating a stable single jet mode that expanded to a maximum of seven jets around the circumference of the emitter slit.

This crown jet formation is attributed to the distribution of charged fluid along the emitter slit, driven by the elevated accelerator voltage. However, when the voltage exceeded 18.5 kV, an imbalance in electric forces between the emitter and accelerator destabilized the jets. This instability reduced the number of jets to three, as shown in Fig. 12(b), and introduced jet width fluctuations resembling a pulsating mode.

This abrupt reduction in jet number may not result solely from charge repulsion, but could also stem from space charge accumulation and local electric field distortion near the emitter slit. These effects can alter the stability of emission sites under high-voltage conditions.

At a higher flow rate of 55 cc/h, the number of cone jets increased compared to 30 cc/h at the same voltage up to 18 kV, although the maximum number of jets remained the same at both flow rates and decreased beyond 18 kV, as shown in Fig. 12(a). Moreover, as the flow rate increased, the voltage required to form the maximum number of jets decreased from 18.5 to 18 kV, as shown in Fig. 12(b). This indicates that higher flow rates allow the maximum number of jets to form at lower voltages, thereby increasing efficiency due to reduced voltage requirements.

In contrast, the capillary emitter generated at most two jets under the 100% mixture (glycerin), ¹² as reported in the previous study, due to limitations in electric field distribution. The formation of up to seven stable jets was only observed in the annular slit-type emitter, highlighting the advantage of the continuous slit geometry for supporting dense and uniform multi-jet emission.

Figures 13 and 14 show the calculated Re and Ca as a function of glycerin concentration for the capillary and annular slit emitters, respectively. The dimensionless values were computed using the fluid properties listed in Table I and the flow rates of 30 and 55 cc/h, based on the respective emitter configurations. The jet velocity was estimated from the known volumetric flow rate and the outlet cross-sectional area of each emitter. However, charge density could not be measured due to equipment limitations. In both cases, the Re decreases and the Ca increases with increasing glycerin concentration. This behavior is driven by the simultaneous increase in viscosity and decrease in surface tension and is consistent across both emitter configurations.

These trends provide physical insight into the role of fluid rheology in multi-jet electrospray behavior. They also form the basis for

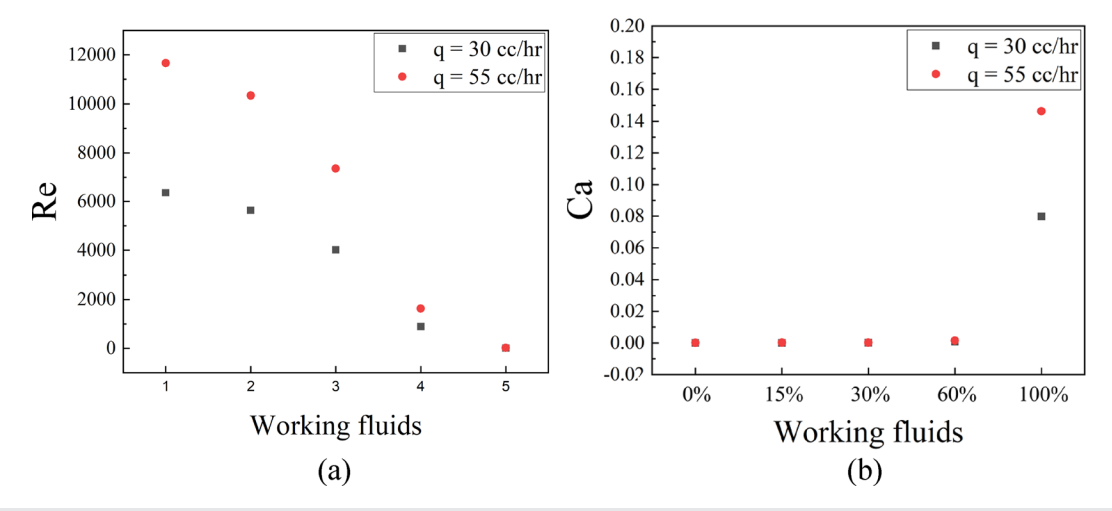


FIG. 13. Calculated dimensionless numbers as a function of mixture ratio for the capillary emitter: (a) Re and (b) Ca.

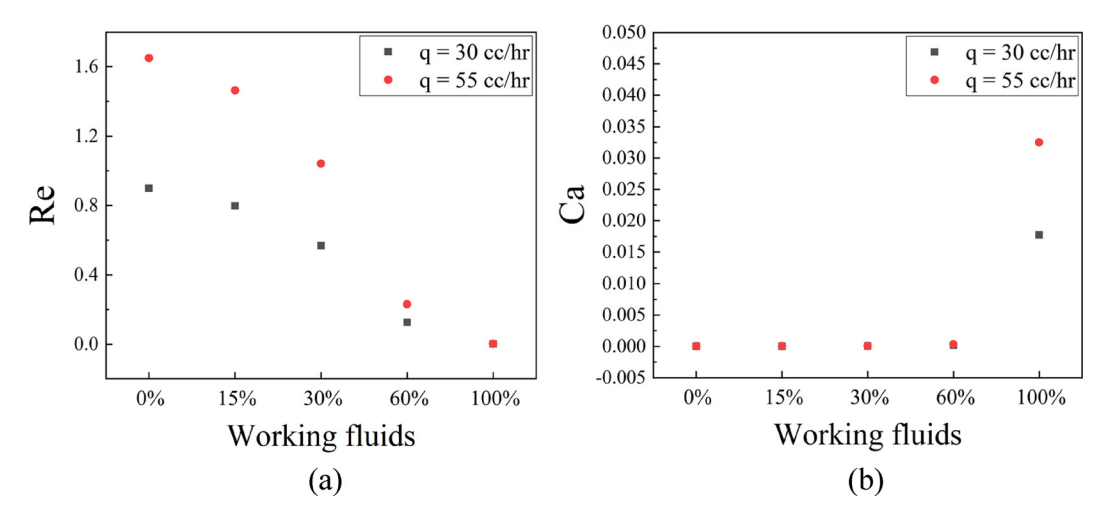


FIG. 14. Calculated dimensionless numbers as a function of mixture ratio for the annular slit emitter: (a) Re and (b) Ca.

interpreting the relationship between Re and the number of jets, as presented in Fig. 15. As shown in Fig. 15, the comparison of the number of jets formed based on voltage and the Re reveals that multi-jet formation occurs only when the Re is below 0.1. This indicates that multi-jet formation does not occur when the inertial force of the fluid is significantly larger than the viscous force. Furthermore, observations of multi-jet formation at different voltages show that the transition region, where the cone–jet first forms, occurs at 13 kV. After this point, from 18 to 18.5 kV, an increase in voltage leads to an increase in the number of jets, defining a stable zone. In contrast, beyond 18–18.5 kV, as the voltage increases, the number of jets decreases, defining an unstable zone. In addition, a maximum of seven jets was observed only for the 100% mixture (glycerin). This is because only the 100% mixture (glycerin) has a Re within the range that allows for multi-jet formation as determined by Eqs. (7)–(9).

In summary, the observed trends in Re and Ca across varying mixture ratios exhibit consistent behavior with classical electrospray theory. The decrease in Re indicates reduced inertial forces, while the increase in Ca reflects stronger viscous dominance. These changes correlate with improved jet stability and are consistent with previously reported electrospray regimes in high-viscosity fluids. The results validate the use of Re and Ca as predictive indicators for multi-jet operation in both capillary and slit-type emitters.

V. CONCLUSION

This study explores the electrospray performance of the annular slit-type emitter, emphasizing the role of viscosity and electric potential in multi-jet formation. By integrating theoretical and experimental findings, the interplay between these parameters in influencing the jet stability and system efficiency is analyzed for advancing the electrospray technology.

Key contributions of this research are summarized:

 Quantitative analysis of multi-jet dynamics of annular slit emitters: This study systematically investigated the relationship between viscosity, electric potential, and multi-jet formation in annular slit-type emitters. The ability to generate up to seven stable jets at optimal conditions marks a significant

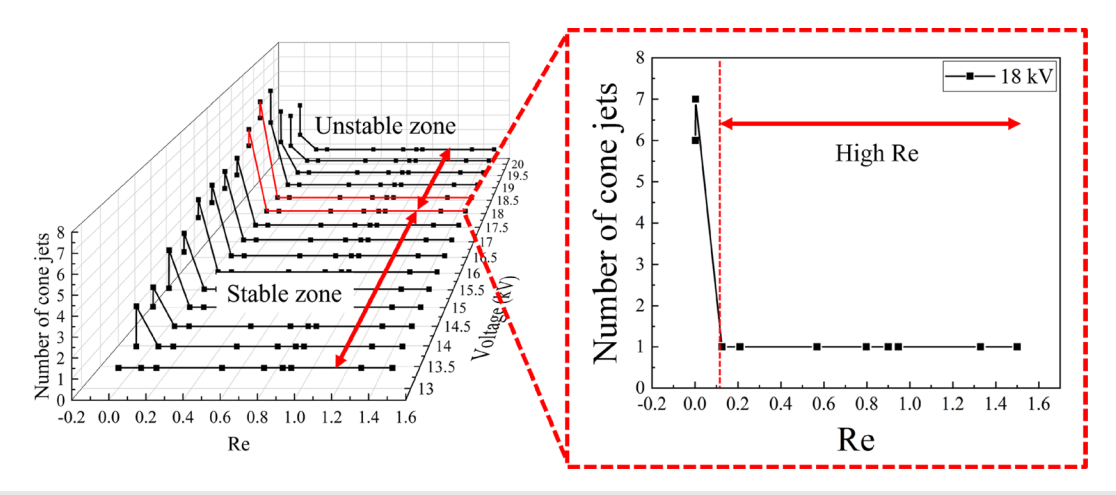


FIG. 15. Comparison of number of cone jets based on Re and voltage

improvement over the mission-proven traditional capillary-type emitters.

- Understanding the effect of viscosity for choosing the ionic propellant: We demonstrated that higher viscosity enhances jet stability by reducing pulsating jet frequency and increasing uniformity. This finding extends the applicability of the Ca and Re framework to the annular slit configuration.
- Optimization of voltage and flow rate of electrospray system: Higher flow rates enabled stable multi-jet formation at lower voltages, enhancing energy efficiency. This finding highlights the annular slit design's scalability and adaptability for various electrospray applications.
- Advanced emitter design for ensuring multi-jet stability: This
 work identified the critical threshold for voltage and viscosity
 beyond which jet instability occurs, providing actionable design
 guidelines for future electrospray systems.

Future research will focus on validating the annular slit-type emitter performance in vacuum conditions and assessing its dynamic compatibility with nanosatellite attitude control systems.

ACKNOWLEDGMENTS

This work was supported by the National Research Foundation of Korea (NRF) Grant No. RS-2024-03357969 contracted through IAAT and IOER of Seoul National University.

Declaration of Generative AI and AI-Assisted Technologies in the Writing Process: During the preparation of this work, the authors used ChatGPT only for the purpose of correcting grammar. After using this tool, the authors reviewed and edited the content as needed and take full responsibility for the content of the published article.

AUTHOR DECLARATIONS Conflict of Interest

The authors have no conflicts to disclose.

Author Contributions

Chanearl Kwon: Formal analysis (equal); Investigation (equal); Methodology (equal); Project administration (equal); Validation (equal); Visualization (equal); Writing – original draft (equal). Sunho Choe: Data curation (equal); Investigation (equal). Jack J. Yoh: Conceptualization (lead); Formal analysis (equal); Funding acquisition (lead); Investigation (equal); Methodology (equal); Project administration (lead); Supervision (lead); Writing – review & editing (lead).

DATA AVAILABILITY

The data that support the findings of this study are available from the corresponding author upon reasonable request.

REFERENCES

- ¹V. E. Krohn, Jr., "Glycerol droplets for electrostatic propulsion," in ARS Electric Propulsion Conference, Berkeley, CA (1962).
- 2S. Mazouffre, "Electric propulsion for satellites and spacecraft: Established technologies and novel approaches," Plasma Sources Sci. Technol. 25, 033002 (2016).

- ³D. O'Reilly, G. Herdrich, and D. F. Kavanagh, "Electric propulsion methods for small satellites: A review," Aerospace 8, 22 (2021).
- ⁴T. Henning, K. Huhn, L. W. Isberner, and P. J. Klar, "Miniaturized electrospray thrusters," IEEE Trans. Plasma Sci. 46, 214–218 (2018).
- ⁵J. Zhang, G. Cai, A. Shahzad, X. Liu, and W. Wang, "Ionic liquid electrospray behavior in a hybrid emitter electrospray thruster," Int. J. Heat Mass Transfer 175, 121369 (2021).
- ⁶D. Villegas-Prados, J. Cruz, M. Wijnen, P. Fajardo, and J. Navarro-Cavallé, "Emission and performance characterization of ionic liquids for an externally wetted electrospray thruster," Acta Astronaut. 219, 97–107 (2024).
- ⁷F. L. Kunze, T. Henning, and P. J. Klar, "3D micro printed capillary electrospray thruster with a fully modular integrated extraction electrode," J. Electr. Propul. 3, 3 (2024).
- ⁸M. Gamero-Castaño and V. Hruby, "Electrospray as a source of nanoparticles for efficient colloid thrusters," J. Propul. Power 17, 977–987 (2001).
- ⁹P. C. Lozano, M. Martínez-Sánchez, and V. Hruby, "Electrospray propulsion," in *Encyclopedia of Aerospace Engineering* (Wiley, 2010).
- ¹⁰K. Lemmer, "Propulsion for cubesats," Acta Astronaut. **134**, 231–243 (2017).
- ¹¹K. Holste, P. Dietz, S. Scharmann, K. Keil, T. Henning, D. Zschätzsch, M. Reitemeyer, B. Nauschütt, F. Kiefer, F. Kunze, J. Zorn, C. Heiliger, N. Joshi, U. Probst, R. Thüringer, C. Volkmar, D. Packan, S. Peterschmitt, K. T. Brinkmann, H. G. Zaunick, M. H. Thoma, M. Kretschmer, H. J. Leiter, S. Schippers, K. Hannemann, and P. J. Klar, "Ion thrusters for electric propulsion: Scientific issues developing a niche technology into a game changer," Rev. Sci. Instrum. 91, 061101 (2020).
- ¹²C. Kwon, U. P. Padhi, P. Kumar, D. Lim, S. Choe, K. Kwon, and J. J. Yoh, "A novel annular slit-type emitter developed for multi-jet electrospray propulsion," Phys. Fluids 36, 027128 (2024).
- ¹³P. Kumar, C. Kwon, K. Kwon, and J. J. Yoh, "On the cone-to-jet transition region and its significance in electrospray propulsion," Acta Astronaut. 205, 12–22 (2023).
- 14 A. Cisquella-Serra, M. Galobardes-Esteban, and M. Gamero-Castaño, "Scalable microfabrication of multi-emitter arrays in silicon for a compact microfluidic electrospray propulsion system," ACS Appl. Mater. Interfaces 14, 43527–43537 (2022).
- 15B. Zhang, H. Liu, B. L. Karger, and F. Foret, "Microfabricated devices for capillary electrophoresis—electrospray mass spectrometry," Anal. Chem. 71, 3258–3264 (1999)
- 16P. R. Patel and D. Haemmerich, "Review on electrospray nanoparticles for drug delivery: Exploring applications," Polym. Adv. Technol. 35, e6507 (2024).
- 17 S. K. Boda, X. Li, and J. Xie, "Electrospraying an enabling technology for pharmaceutical and biomedical applications: A review," J. Aerosol Sci. 125, 164–181 (2018)
- ¹⁸M. Gamero-Castaño and A. Cisquella-Serra, "Electrosprays of highly conducting liquids: A study of droplet and ion emission based on retarding potential and time-of-flight spectrometry," Phys. Rev. Fluids 6, 013701 (2021).
- ¹⁹A. Quraishi, S. Dworski, C. N. Ryan, A. Ferreri, G. Vincent, A. Croos, A. Wild, and E. Neubauer, "Designing and commercialization of porous emitter electrospray thruster for space applications," in AIAA SCITECH 2023 Forum 0262 (2023).
- ²⁰N. S. Mühlich, J. Gerger, B. Seifert, and F. Aumayr, "Performance improvements of IFM Nano Thruster with highly focused ion beam generated with a compact electrostatic lens module," Acta Astronaut. 201, 464–471 (2022).
- ²¹R. S. Legge, Jr. and P. C. Lozano, "Electrospray propulsion based on emitters microfabricated in porous metals," J. Propuls. Power 27, 485–495 (2011).
- ²²D. Krejci and A. Reissner, "The first 100 FEEP propulsion systems in space: A statistical view and lessons learnt of 4 years of ENPULSION," in *IEPC-2022–199*, 37th International Electric Propulsion Conference (Electric Rocket Propulsion Society, 2022).
- ²³J. Mitterauer, "Indium: An alternative propellant for FEEP-thrusters," in 37th Joint Propulsion Conference and Exhibit (AIAA, 2001), p. 3792.
- ²⁴T. Schönherr, B. Little, D. Krejci, A. Reissner, and B. Seifert, "Development, production, and testing of the IFM nano FEEP thruster," in 36th International Electric Propulsion Conference (Electric Rocket Propulsion Society, 2019), pp. 1–11.
- 25 R. S. Legge, P. Lozano, and M. Martinez-Sanchez, "Fabrication and characterization of porous metal emitters for electrospray thrusters," in 30th International Electric Propulsion Conference (Electric Rocket Propulsion Society, 2007), p. 145.
- ²⁶J. Mitterauer, "Emission performance of a slit type caesium field ion source," J. Phys. Colloq. **50**, C8-196 (1989).

- ²⁷D. R. Valentian, C. M. Bartoli, H. A. Pfeffer, H. J. H. V. Rohden, and D. Stewart, "Field-emission ion source and ion thruster apparatus comprising such sources," U.S. Patent No. 4,328,667 (1982).
- such sources," U.S. Patent No. 4,328,667 (1982).

 28 M. Tajmar, A. Genovese, N. Buldrini, and W. Steiger, "Miniaturized indium-FEEP multiemitter design and performance," in NanoTech 2002-"At Edge Revolution" AIAA Paper No. 2002-5718 (2002).
- Revolution" AIAA Paper No. 2002-5718 (2002).

 29 A. D. Ketsdever and M. M. Micci, *Micropropulsion for Small Spacecraft*, 1st ed. (American Institute of Aeronautics and Astronautics, Inc., Reston, VA, 2000), Chap. 3.
- 30R. C. Weast, Handbook of Chemistry and Physics (CRC Press Inc., Cleveland, 1974).
- ³¹F. M. White, Fluid Mechanics, 8th ed. (McGraw-Hill Interamericana de España S.L., 2015).
- 32J. Mitterauer, "Field emission electric propulsion: Emission site distribution of slit emitters," IEEE Trans. Plasma Sci. 15, 593–598 (1987).
- ³³Y. Emir, T. Suzuki, K. Ito, G. J. Gotama, W. Anggono, and M. Ichiyanagi, "Analysis of the spray characteristics of water and water/glycerin mixtures using an interferometric laser imaging for droplet sizing technique," Int. J. Technol. 12, 101–112 (2021).
- 34P. M. Meaney, C. J. Fox, S. D. Geimer, and K. D. Paulsen, "Electrical characterization of glycerin: Water mixtures: Implications for use as a coupling medium in microwave tomography," IEEE Trans. Microwave Theory Tech. 65, 1471–1478 (2017).